Electrochemical investigation of corrosion inhibition of AA6063 alloy in 1M hydrochloric acid using Schiff base compounds.

Sanaulla Pathapalya Fakrudeen[1], Lokesh H. B[2], Ananda Murthy H. C[3], Bheema Raju V.[4]

[1]Department of Engineering Chemistry, HKBK College of Engineering, Nagawara, Bangalore -560045, Karnataka, India.
[2]Department of Engineering Chemistry, Vivekananda Institute of Technology, , Bangalore-560074, India.
[3]Department of Engineering Chemistry, R N Shetty Institute of Technology, Bangalore-560061, Karnataka, India.
[4]Department of Engineering Chemistry, Dr. Ambedkar Institute of Technology,, Bangalore – 560056, India.

Abstract: *The electrochemical behavior of aluminium alloy AA6063 were investigated using Schiff base compounds namely N, N'-bis (Salicylidene)-1, 2-Diaminoethane(Salen) and N, N'-bis (3-Methoxy Salicylidene)-1, 2 Diaminoethane (Msalen) as corrosion inhibitors in presence of 1M Hydrochloric Acid by Potentiodynamic polarization(PDP), electrochemical impedance spectroscopy(EIS) and weight loss method. Potentiodynamic polarization study revealed that the two Schiff bases acted as mixed type inhibitors. The change in EIS parameters is indicative of adsorption of Schiff bases on aluminum alloys surface leading to formation of protective layer. The weight loss study showed that the inhibition efficiency of these compounds increases with increase in concentration and vary with solution temperature and immersion time. The thermodynamic parameters were also calculated to investigate the mechanism of corrosion inhibition. The effect of methoxy group on corrosion efficiency was observed from the results obtained between Salen and Msalen. The effectiveness of these inhibitors were in the order of Msalen>Salen. The adsorption of Schiff bases on AA6063 alloy surface in acid obeyed Langmuir adsorption isotherm. The surface characteristics of inhibited and uninhibited alloy samples were investigated by scanning electron microscopy (SEM).*

Keywords: *Corrosion inhibitors, Schiff base, Electrochemical techniques, Adsorption isotherms, Aluminum alloy.*

I. Introduction

Aluminum alloys are important structural metals, particularly in the aerospace and automobile industry. Pure aluminum metal is corrosion resistant due to formation of passive film on the metal surface. However, pure aluminum metal does not possess adequate strength for most aerospace, automobile and industrial applications and must be alloyed with other metals, notably copper, magnesium, silicon, iron, zinc and other minor constituent. These alloys are classified by a numbering system that reflects both the chemical composition and the heat treatment (tempering) of the alloy [1-2].

It has been reported that the cost due to corrosion in many countries is as high as 5% of the GNP [3]. This represents a huge amount of money which should have been channeled into the provision of basic social amenities in these countries. In practice corrosion can never be stopped but can be controlled to a reasonable level. Corrosion of aluminum and its alloys has been a subject of numerous studies due to their high technological value and wide range of industrial applications. Aluminum alloys, however, are reactive materials and are prone to corrosion. Aluminum alloys form a compact, strongly adherent and continuous passive oxide film on surface upon exposure to the atmosphere or aqueous solutions. However the surface film is amphoteric and dissolves substantially when the metal is exposed to high concentrations of acids or bases [4].

In order to combat the corrosion of metals, several techniques have been applied. The use of inhibitors is one of the most practical methods for protection against corrosion in acidic media. Generally, the organic compounds containing hetero atoms such as N, O, S, Se etc. are found to have function as very effective corrosion inhibitors [5-10]. The corrosion inhibition efficiency of organic compounds is related to their adsorption properties. Adsorption depends on the nature of the metal surface, type of corrosive medium and the chemical structure of the inhibitor [11]. Studies report that the adsorption of the organic inhibitors mainly depends on some physicochemical properties of the molecule, related to its functional groups.

. The aim of this study is to investigate the inhibition effect of some Schiff base compounds N, N'-bis (Salicylidene)-1, 2-Diaminoethane(Salen) and N, N'-bis (3-Methoxy Salicylidene)-1, 2 Diaminoethane (Msalen) on the corrosion of AA6063 alloy in 1M HCl using weight loss, potentiodynamic polarization and electrochemical impedance spectroscopy techniques. The mode of adsorption and the corrosion inhibition

mechanism are also discussed. The surface morphology was investigated by scanning electron microcopy (SEM).

The inhibition effect of Schiff base compounds are reported on steel [12-13.], Copper [14-15], and pure aluminium and its alloys [16- 20], in acidic medium. However, no substantial work has been carried out on corrosion inhibition of aluminium alloys in acidic medium by Schiff bases. Thus, it was thought worthwhile to study the corrosion inhibition effect of Schiff base compounds namely N, N'-bis (Salicylidene)-1, 2-Diaminoethane (Salen) and N, N'-bis (3-Methoxy Salicylidene)-1, 2 Diaminoethane (Msalen)) on AA6063 Alloy in 1M Hydrochloric acid medium.

II. Materials and Methods

2.1 Materials

The alloy samples were procured from M/S. Fenfe Metallurgical, Bangalore, India. The typical chemical composition of AA6063 alloy in weight percentage is magnesium (0.45-0.9), silicon (0.2-0.60), copper (0.1), iron (0.35max), manganese (0.1max), titanium (0.1 Max) chromium (0.10), zinc (0.1 max) and aluminum (balance) [21].

The alloy samples were cut into cylindrical test specimens and moulded in cold setting Acrylic resin exposing a surface area of 1.0 cm^2 for electrochemical measurements. For weight loss experiments the cylindrical alloy rods were cut into 24 mm dia x 2mm length -circular cylindrical disc specimens using an abrasive cutting wheel and a 2mm mounting hole at the centre of the specimen was drilled. Before each experiment, the electrodes were abraded with a sequence of emery papers of different grades (600, 800, and 1200), washed with double distilled water, degreased with acetone and dried at 353 K for 30 min in a thermostated electric oven and stored in a moisture-free desiccator prior to use. The corrosive medium selected for this study was 1M hydrochloric acid, which was prepared from analytical grade 37 percent acid concentrated (Merck) in double distilled water.

2.2 Inhibitor.

The Schiff Bases were prepared by the condensation of respective aromatic aldehydes with each of diamines as per the reported procedure [22]. All reagents used were of analytical grade procured from Sigma Aldrich. N,N'-bis(Salicylidene)-1,2-Diaminoethane (Salen) was prepared by slow addition of Salicylaldehyde (2 mmol) in 30 mL methanol over a solution of 1,2-diaminoethane (1mmol) in 30 mL methanol and N,N'-bis(3-MethoxySalicylidene)-1,2-Diaminoethane (Msalen) by slow addition of Methoxysalicylaldehyde (2 mmol) in 30 mL methanol over a solution of 1,2-diaminoethane (1 mmol) in 30 mL methanol taken in a 250 mL condensation flask. In each case, 2-3drops of acetic acid was added to the mixture of aldehyde and diamine with stirring at constant temperature 298K for 1 hour. Further the mixture was refluxed for 4-5 hours on a water bath, heating occasionally to improve the yield of the product. The reaction mixture was cooled to room temperature overnight and the colored compound was filtered off and dried. The compounds were recrystallised with ethanol. The product identity was confirmed *via* melting points, Fourier transform infrared spectroscopy (FT-IR) and Proton Nuclear Magnetic Resonance (^{1}H NMR). The structure, molecular formula, molecular mass, melting points are shown in Table-1.

N,N'-bis(Salicylidene)-1,2-Diaminoethane
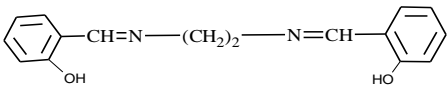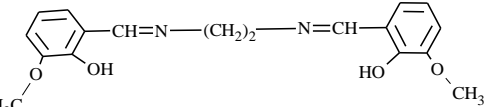IR (KBr cm^{-1}): 3415(OH), 3040(=C-H), 2860(-CH), 1628(C=N).
^{1}HNMR (CDCl$_3$): δ 3.94 (s, 4H,-CH$_2$-N), 6.83–7.3 (m, 8H, ArH). 8.35(s, 2H, N=CH), 13.17 (s, 1H, OH),
N,N'-bis(3-Methoxy Salicylidene)-1,2-Diaminoethane
IR (KBr cm^{-1}): 3443(OH), 3004(=C-H), 2896(-CH), 1628(C=N). 1246(-OCH$_3$)
^{1}HNMR (CDCl$_3$): δ 3.88(s, 6H, -OCH$_3$), δ 3.96 (s, 4H,-CH$_2$-N), 6.75–6.91 (m, 6H, ArH). 8.33(s, 2H, N=CH), 13.56 (s, 1H, OH),

Table-1. Schiff Bases

Structure and Name	Molecular Formula	Molecular Mass	Melting Point
N,N'-bis(Salicylidene)-1,2-Diaminoethane **(Salen)**	C$_{16}$H$_{16}$N$_2$O$_2$	268.31	129°C
N,N'-bis(3-MethoxySalicylidene)-1,2-Diaminoethane (M-Salen)	C$_{18}$H$_{20}$N$_2$O$_4$	328.37	180°C

2.3 Electrochemical measurements.

Potentiodynamic polarization (PDP) and electrochemical impedance spectroscopy (EIS) measurements were performed using CH660c electrochemical work station. All electrochemical experiments were measured after immersion of alloy specimens for 30 minutes to establish a steady state open circuit potential in absence and presence of inhibitors at 303 K.

Tafel plots were obtained using conventional three electrode Pyrex glass cell with alloy specimen ($1 cm^2$) as working electrode (WE), platinum electrode (Pt) as an auxiliary electrode and standard calomel electrode (SCE) as reference electrode. All the values of potential were referred to SCE. Tafel plots were obtained by polarizing the electrode potential automatically from -250 to $+250$ mV with respect to open circuit potential (OCP) at a scan rate $1 mV\ s^{-1}$. The linear Tafel segments of anodic and cathodic curves were extrapolated to corrosion potential (E_{corr}) to obtain corrosion current densities (I_{corr}). The inhibition efficiency was evaluated from the I_{corr} values using the following relationship (1):

$$\mu_p\% = \frac{i^0_{corr} - i_{corr}}{i^0_{corr}} \times 100 \tag{1}$$

Where, i^0_{corr} and i_{corr} are values of corrosion current densities in absence and presence of inhibitor respectively.

EIS measurements were carried out in a frequency range from 100 kHz to 0.01 Hz with small amplitude of 10mV peak -to-peak, using AC signal at OCP. The impedance data was analyzed using Nyquist plot and Echem software ZSimpWin version 3.21 was used for data fitting. The inhibition efficiency (μR_{ct} %) was calculated from the charge transfer resistance (R_{ct}) values using following equation (2):

$$\mu_{Rct}\% = \frac{R^i_{ct} - R^0_{ct}}{R^i_{ct}} \times 100 \tag{2}$$

Where, R^0_{ct} and R^i_{ct} are the charge transfer resistance in absence and presence of inhibitor, respectively.

2.4 Weight loss measurements

Weight loss measurements were performed on aluminium alloys as per ASTM Method [23]. The test specimens were immersed in 100mL 1M hydrochloric acid solution in absence and presence of different concentrations (25,50,75 and 100 ppm) of Salen and Msalen at different temperature ranges (303, 313, 323 and 333 K) in thermostated water bath. The difference in weight for exposed period of 2, 4, 6 and 8 hours was taken as the total weight loss. The weight loss experiments were carried out in triplicate and average values were recorded. The corrosion rate was evaluated as per ASTM Method [23]. The percentage of inhibition efficiency ($\mu_{WL\%}$) and the degree of surface coverage (θ) were calculated using equations (3) and (4):

$$\mu_{WL}\% = \frac{Wo - Wi}{Wo} \times 100 \tag{3}$$

$$\theta = \frac{Wo - Wi}{Wo} \tag{4}$$

Where W_O and Wi are the weight loss values of aluminium alloy sample in the absence and presence of the inhibitor and θ is the degree of surface coverage of the inhibitor.

2.5 Scanning electron microscopy (SEM).

The surface morphology of the corroded surface in the presence and absence of inhibitors were studied using scanning electron microscope [Model No JSM-840A-JEOL]. To understand the morphology of the aluminium alloy surface in the absence and presence of inhibitors, the following cases were examined.
(i) Polished aluminium alloy specimen. (ii) Aluminium alloy specimen dipped in 1M HCl. (iii) Aluminium alloy specimen dipped in 1M HCl containing 100 ppm of Schiff base.

III. Results and Discussion

3.1 Potentiodynamic polarisation (PDP)

The polarization measurements of AA6063 alloy specimens were carried out in 1M Hydrochloric acid, in the absence and in the presence of different concentrations (25 -100 ppm) of Salen and Msalen at 303K in order to study the anodic and cathodic reactions. The Fig.1 (a) and (b) represents potentiodynamic polarisation curves (Tafel plots) of AA6063 alloy in 1M Hydrochloric acid in absence and presence of various concentrations of Salen and Msalen at 303K respectively. The electrochemical parameters i.e. corrosion potential (E_{corr}), corrosion current density (i_{corr}), cathodic and anodic Tafel slopes (b_a and b_c) associated with the polarization measurements of Salen and Msalen are listed in Table.2. The inhibition efficiency (μ_p %) of inhibitors at different concentrations was calculated from the equation (1). It is observed from the PDP results that, in presence of inhibitors, the curves are shifted to lower current density (i_{corr}) regions and Tafel slopes b_a and b_c values increased with increase in concentration of inhibitors showing the inhibition tendency of Salen and Msalen. The corrosion potential (E_{corr}) values do not show any appreciable shift, which suggest that both inhibitors acted as mixed type but predominantly cathodic inhibitors [24-25]. This can probably be due to the adsorption of protonated Schiff base molecules on the cathodic and anodic sites.
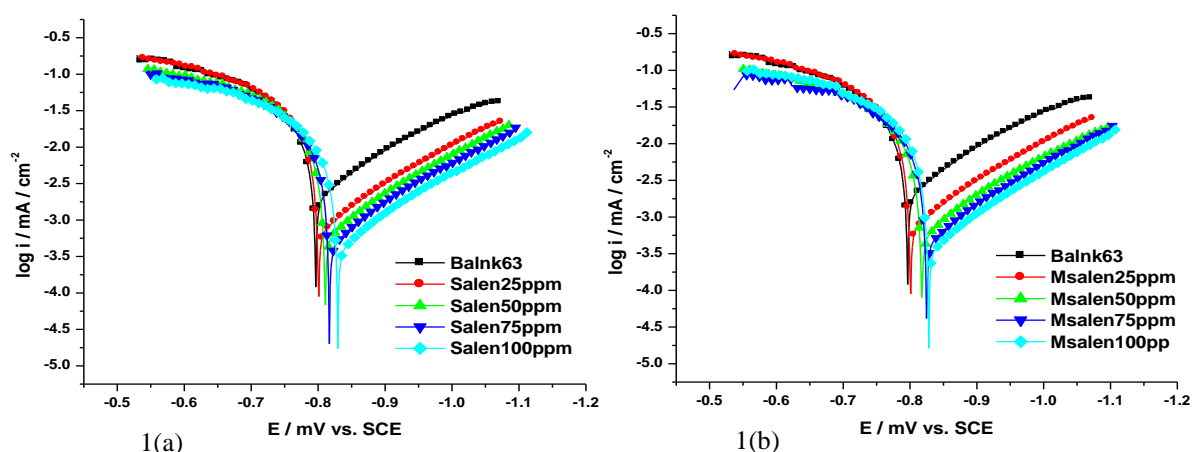

Figure. 1. Potentiodynamic polarisation curves (Tafel plots) of AA6063 alloy in 1M Hydrochloric acid in absence and presence of various concentrations of (a) Salen and (b) Msalen at 303K.

Table.2. Potentiodynamic polarisation parameters of AA6063 alloy in 1M Hydrochloric acid in absence and presence of various concentrations of (a) Salen and (b) Msalen at 303K.

Tafel data						
Inhibitor	Concentration (ppm)	$-E_{corr}$ (mV vs. SCE)	i_{corr} (mA cm^{-2})	b_c (mV dec^{-1})	b_a (mV dec^{-1})	$\mu_p\%$
Salen	0	797	3.29	187	47	---
	25	801	1.12	188	51	65.9
	50	810	1.01	194	52	69.3
	75	816	0.92	197	55	72.0
	100	829	0.82	201	57	75.0
Msalen	25	807	1.05	192	54	68.1
	50	818	0.88	195	56	73.3
	75	825	0.82	199	59	75.1
	100	828	0.72	205	61	78.1

3.2 Electrochemical impedance spectroscopy.

The effect of the inhibitor concentration on the impedance behavior of AA6063 alloy in 1M Hydrochloric acid was studied and Nyquist plots of AA6063 in absence and presence of various concentrations of Schiff bases are given in Fig 2 (a) and (b). It is clear from the Figr that the impedance diagrams obtained yield a semicircle shape. This indicates that the corrosion process is mainly controlled by charge transfer. The general shape of the Nyquist plots is similar for all samples of AA 6063 alloy, with a large capacitive loop at higher frequencies and inductive loop at lower frequencies. The similar impedance plots have been reported for

the corrosion aluminum and its alloys in hydrochloric acid [26-32]. The Nyquist plot with a depressed semicircle with the center under the real axis is characteristic property of solid electrode and this kind of phenomenon is known as the dispersing effect [33-34].
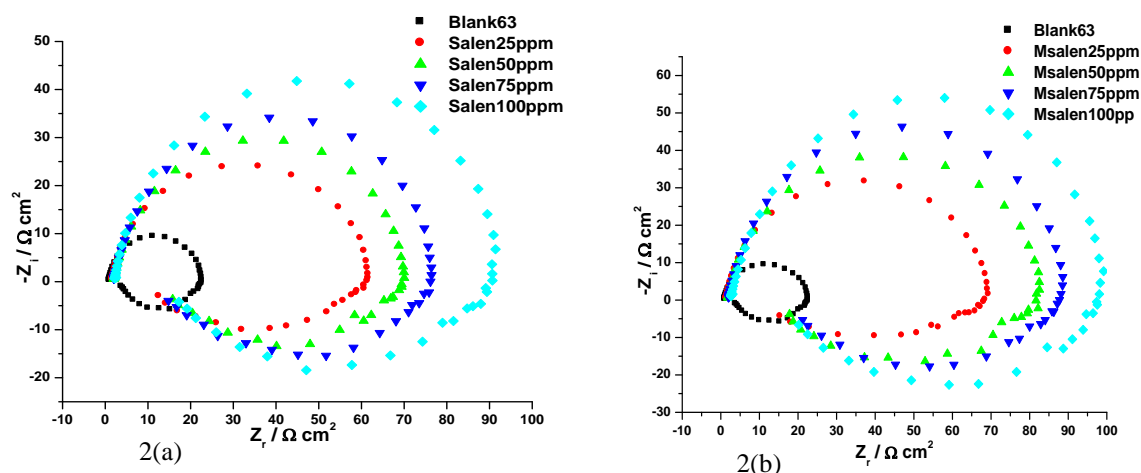

Figure. 2. Nyquist plot for AA6063 alloy in 1M Hydrochloric acid in absence and presence of various concentrations of (a) Salen and (b) Msalen at 303K

An equivalent circuit fitting of five elements was used to simulate the measured impedance data of AA6063 alloy is depicted in Fig.3.
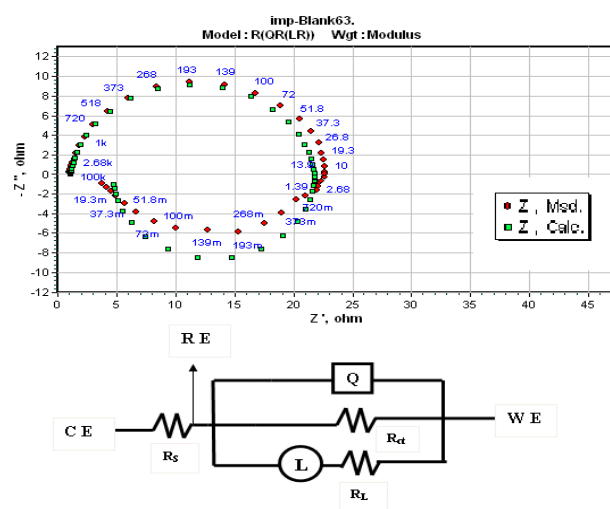

Figure. 3. The equivalent circuit model used to fit the experimental impedance data

The equivalent circuit includes solution resistance R_s, charge transfer resistance R_{ct}, inductive elements R_L and L. The circuit also consists of constant phase element, CPE (Q) in parallel to the parallel resistors R_{ct} and R_L, and R_L is in series with the inductor L. The impedance spectra for the aluminium alloy in absence and presence of the inhibitors are depressed. The deviation of this kind is referred as frequency dispersion, and has been attributed to inhomogeneous of solid surface of aluminum alloy. Assumption of a simple R_{ct} –C_{dl} is usually a poor approximation especially for systems showing depressed semicircle behavior due to non – ideal capacitive behaviour of solid electrodes [35]. The capacitor in the equivalent circuit can be replaced by a constant phase element (CPE), which is a frequency dependent element and related to surface roughness. CPE is substituted for the respective capacitor of C_{dl} in order to give a more accurate fit. The impedance function of a CPE is defined in impedance [36] representation as (5).

$$Z_{CPE} = \frac{1}{(Y_0 j\omega)^n} \qquad (5)$$

Where, Y_0 magnitude of CPE, n is exponent of CPE, and are frequency independent, and ω is the angular frequency for which $-Z''$ reaches its maximum value, n is dependent on the surface morphology : $-1 \leq n \leq 1$. Y_0 and n can be calculated by the equation proved by Mansfeld et al [37]. The double layer capacitance (C_{dl}) can be calculated from the equation.(6) [38].

$$C_{dl} = Y_0 \, (\omega_{max})^{\,n-1} \qquad\qquad (6)$$

Where C_{dl} is the double layer capacitance and ω_{max} is the angular frequency at which $-Z''$ reaches maximum and n is the CPE exponent.

The electrochemical impedance parameters R_s, R_{ct}, R_L, L, ω, CPE, n and C_{dl} are listed in Table-3.The inhibition efficiency was evaluated by R_{ct} and C_{dl} values of the impedance data, it is shown from Table-3 that charge transfer resistance (R_{ct}) of inhibited system increased and double layer capacitance (C_{dl}) decreased with increase in inhibitor concentration. This was due to adsorption of Schiff base molecule on the metal surface, the adsorbed inhibitor blocks either cathodic or anodic reaction or both formation of physical barrier, which reduces metal reactivity. The effect of inhibitor may be due to changes in electric double layer at the interface of solution and metal electrode. The decrease in double layer capacitance (C_{dl}) can be caused by decrease in local dielectric constant and /or increase in the thickness of electric double layer, this suggest that the Schiff base molecules inhibit the aluminium alloy by adsorption at the metal – acid interface. It is evident that the inhibition efficiency increases with increase in inhibitor concentration which is in good agreement with the Potentiodynamic polarization results.

Table-3. Electrochemical impedance parameters of AA6063 alloy in 1M Hydrochloric acid in absence and presence of various concentrations of (a) Salen and (b) Msalen at 303K

EIS data										
Inhibitor	Concentration (ppm)	R_S ($\square$ cm^2)	R_{ct} ($\square$ cm^2)	R_L ($\square$ cm^2)	L (H cm^{-2})	$\square$ (Hz)	CPE (µF cm-2)	n	Cdl (µF cm^{-2})	µ Rct %
Salen	0	1.06	21	4.3	24.5	9.4	71.0	0.9225	52.0	---
	25	1.09	61	23.4	131	23	41.0	0.8970	24.6	65.6
	50	1.13	69	24,7	152	29	38.0	0.9080	23.5	69.6
	75	1.17	77	27.4	157	35	36.1	0.9161	22.9	72.7
	100	1.21	91	28.3	167	41	30.1	0.9266	20.0	76.9
Msalen	25	1.15	68	27.8	136	31	36.7	0.8687	18.4	69.1
	50	1.18	82	31.2	205	38	29.0	0.9077	17.5	74.4
	75	1.24	88	35.0	225	46	25.0	0.9145	15.4	76.6
	100	1.29	98	35.7	263	55	21.7	0.9161	13.3	78.6

3.3 Weight loss measurements

The experimental data of weight loss (Δw), percentage of inhibition efficiency ($\mu_{WL}\%$), Corrosion Rate (C.R.) in mmpy and degree of Surface Coverage (θ) for AA6063 in 1M Hydrochloric acid in absence and presence of various concentration of (a) Salen and (b) Msalen Schiff bases at 2 hours of exposure time and different temperature are shown in Table. 4.

3.3.1 Effect of inhibitor concentration

The variation of inhibition efficiency ($\mu_{WL}\%$) with inhibitor concentration is shown in Fig..4(a). Increase in inhibition efficiency at higher concentration of inhibitor may be attributed to larger coverage of metal surface with inhibitor molecules. The maximum inhibition efficiency was achieved at 100 ppm and a further increase in inhibitor concentration caused no appreciable change in performance

3.3.2 Effect of immersion time

The effect of immersion time on inhibition efficiency is shown in Fig. 4(b). All the tested Schiff bases show a decrease in inhibition efficiency with increase in immersion time from 2 to 8 hours. This indicates desorption of the Schiff Base over a longer test period and may be attributed to various other factors such as formation of less persistent film layer on the metal surface, and increase in cathodic reaction or increase in ferrous ion concentration [39].

3.3.3 Effect of temperature

The influence of temperature on inhibition efficiency of two Schiff bases compounds is shown in Fig.4(c). The inhibition efficiency for the two Schiff base compounds decreases with increase in temperature from 303 to 333K. The decrease in inhibition efficiency with rise in temperature may be attributed to desorption of the inhibitor molecules from metal surface at higher temperatures and higher dissolution rates of aluminium at elevated temperatures.

Table- 4. Weight loss parameters for AA6063 in 1M hydrochloric acid in the absence and presence of various concentrations of Salen and Msalen at 2 hours of exposure time and different temperature.

	Inhibitor	Conc /ppm	Weight Loss(Δw) / mg, Percentage of Inhibition (μ_{WL}%), Corrosion Rate(CR) / mmpy, Surface Coverage(θ)														
		303 K				313 K				323 K				333 K			
		Δw	μ_{WL}%	CR	θ	Δw	μ_{WL}%	CR	θ	Δw	μ_{WL}%	CR	θ	Δw	μ_{WL}%	CR	θ
Salen	Blank	13.7	----	21.0	----	49.9	---	76.4	---	102.8	----	157.3	---	199.8	----	305.8	----
	25	4.7	66	7.1	0.66	21.5	57	32.8	0.57	54.5	47	83.4	0.47	117.9	41	180.4	0.41
	50	4.1	70	6.3	0.7	20.0	60	30.5	0.6	50.4	51	77.1	0.51	109.9	45	168.2	0.45
	75	3.7	73	5.7	0.73	18.5	63	28.3	0.63	47.3	54	72.4	0.54	103.9	48	159.0	0.48
	100	3.3	76	5.0	0.76	16.0	68	24.4	0.68	42.1	59	64.5	0.59	95.9	52	146.8	0.52
Msalen	25	4.4	68	6.7	0.68	20.0	60	30.5	0.6	49.3	52	75.5	0.52	109.9	45	168.2	0.45
	50	3.8	72	5.9	0.72	17.5	65	26.7	0.65	45.2	56	69.2	0.56	101.9	49	155.9	0.49
	75	3.2	77	4.8	0.77	16.5	67	25.2	0.67	42.1	59	64.5	0.59	91.9	54	140.7	0.54
	100	2.9	79	4.4	0.79	14.5	71	22.1	0.71	36.0	65	55.1	0.65	81.9	59	125.4	0.59

4(a)　　　　　　4(b)　　　　　　4(c)
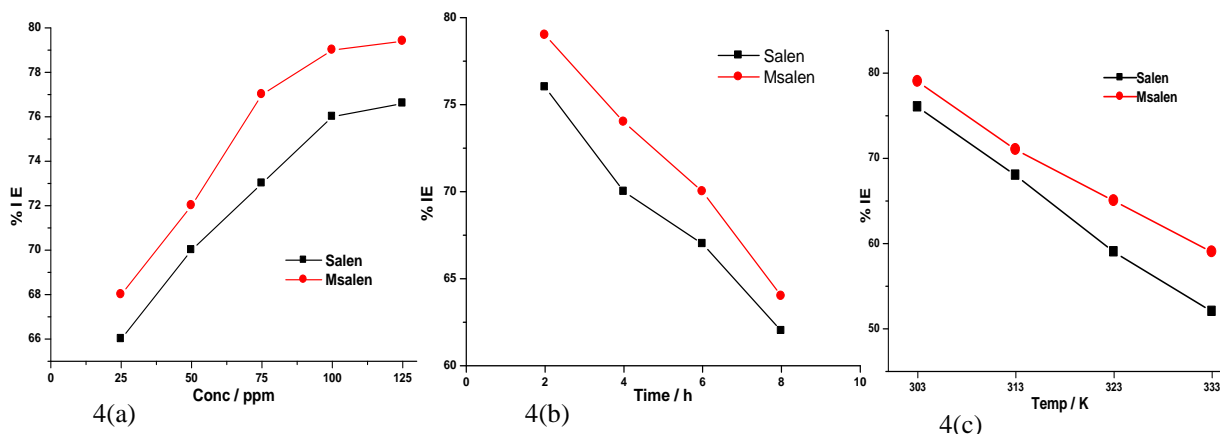
Figure. 4. Variation of inhibition efficiency with (a) Inhibitor concentration (b) Exposure time (c) Temperature in 1M Hydrochloric acid for Salen and Msalen.

3.3.4 Thermodynamic activation parameters

Thermodynamic activation parameters are important to study the inhibition mechanism. The activation energy (Ea) is calculated from the logarithm of the corrosion rate in acidic solution is a linear function of (1/T) - Arrhenius equation (7):

$$\log (CR) = -E_a / 2.303RT + A \qquad (7)$$

Where, Ea is the apparent effective activation energy, R is the universal gas constant and A is the Arrhenius pre exponential factor. Plots of logarithm of corrosion rate obtained by weight loss measurement versus 1/T gave straight lines and slope equal to ($-E_a/2.303R$) as shown in Figs. 5(a) and 5(b) for Salen and Msalen respectively. The E_a values calculated are listed in Table-5.
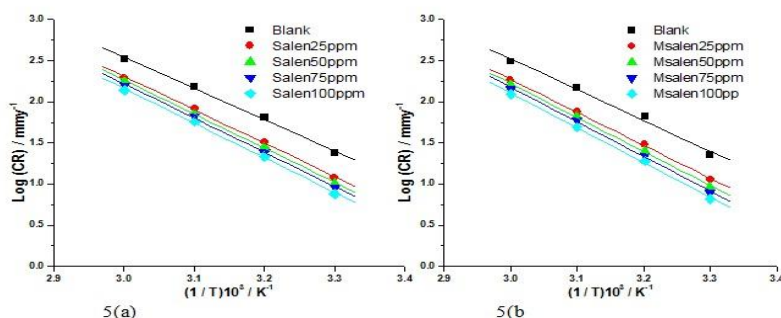
Figure. 5. Arrhenius plot of log CR versus 1/T in absence and presence of (a) Salen and (b)Msalen.

A plot of log (CR/T) versus 1/T gave a straight line, Figs. 6(a) and (b) with a slope of $(-\Delta H/2.303\ R)$ and an intercept of $[(\log (R/Nh) + (\Delta S/2.303\ R)]$, from which the values of ΔS^* and ΔH^* were calculated. The straight lines were obtained according to transition state equation (8):

$$C\ R = RT/\ N\ h\ \exp(-\Delta H^*/\ RT) \exp(\Delta S^*/\ R) \qquad (8)$$

Where, h is the Plank constant, N is the Avogadro number, ΔS^* is entropy of activation and ΔH^* is the enthalpy of activation. The ΔS^* and ΔH^* values calculated are listed in Table-5.
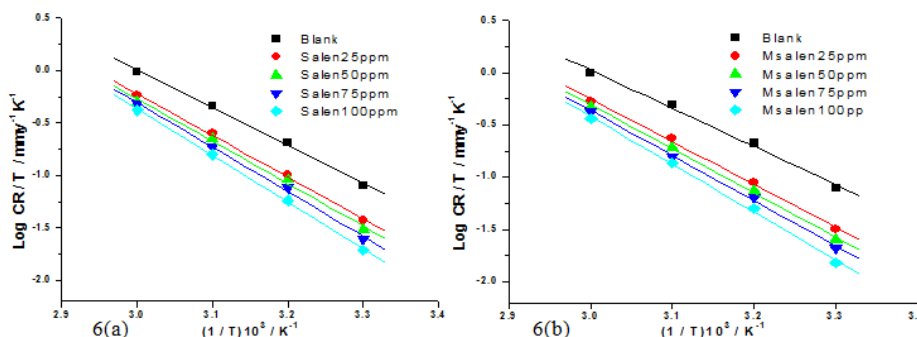

Figure. 6. Arrhenius plot of log (CR/T) versus 1/T in absence and presence of (a) Salen and (b) Msalen.

Table-5 Thermodynamic parameters of activation of AA6063 in 1M HCl in presence and absence of different concentrations of Salen and Msalen.

Inhibitor	Concentration (ppm)	E_a (kJmol^{-1})	ΔH^* (kJmol^{-1})	ΔS^* (J mol^{-1} K^{-1})
Salen	0	72.49	69.22	10.22
	25	77.78	76.07	26.38
	50	79.43	77.58	29.98
	75	79.79	81.40	40.79
	100	80.92	84.84	49.91
Msalen	25	76.84	78.17	32.07
	50	79.23	80.81	38.97
	75	80.62	82.75	43.75
	100	80.93	87.71	57.54

The E_a values of aluminium alloy in 1M Hydrochloric acid in the presence of Schiff base compounds are higher than those in the absence of Schiff bases. The increase in the E_a values, with increasing inhibitor concentration is attributed to physical adsorption of inhibitor molecules on the metal surface [40]. In other words, the adsorption of inhibitor on the electrode surface leads to formation of a physical barrier that reduces the metal dissolution in electrochemical reactions [41]. The inhibition efficiency decreases with increase in temperature which indicates desorption of inhibitor molecules as the temperature increases [42]. The values of enthalpy of activation (ΔH^*) are positive; this indicates that the corrosion process is endothermic. The values of entropy of activation (ΔS^*) are higher in the presence of inhibitor than those in the absence of inhibitor. The increase in values of ΔS^* reveals that an increase in randomness occurred on going from reactants to the activated complex [43-45].

3.3.5 Adsorption isotherms

It is generally assumed that the adsorption of the inhibitor at the interface of metal and solution is the first step in the mechanism of inhibition aggressive media. It is also widely acknowledged that adsorption isotherms provide useful insights into the mechanism of corrosion inhibition. The investigated compounds inhibit the corrosion by adsorption at the metal surface. Theoretically, the adsorption process has been regarded as a simple substitution adsorption process, in which an organic molecule in the aqueous phase substitutes the water molecules adsorbed on the metal surface [46]. The surface coverage (θ) value calculated from weight loss data for different concentrations of Schiff bases was used to explain the best adsorption isotherm. The value of surface coverage (θ) was tested graphically for fitting a suitable adsorption isotherm. Attempts were made to fit surface coverage (θ) values of various isotherms including Langmuir, Freundlich and Temkin isotherms. Among three adsorption isotherms obtained, the best fitted isotherm was the Langmuir adsorption isotherm ($C_{(inh)} / \theta$ vs. $C_{(inh)}$) Fig.7(a) with the linear regression coefficient values (R^2) in the range of 0.9994 - 0.9995. The Langmuir adsorption isotherm can be expressed by following equation (9):

$$\frac{C_{(inh)}}{\theta} = \frac{1}{K_{(ads)}} + C_{(inh)} \qquad (9)$$

Where $C_{(inh)}$ is inhibitor concentration and $K_{(ads)}$ is an equilibrium constant for adsorption and desorption.
The $K_{(ads)}$ was calculated from the intercepts of the straight lines on the $C_{(inh)} / \theta$ axis Fig.7(a) and standard free energy of adsorption of inhibitor ΔG^0_{ads} was calculated using the relation (10);.

$$\Delta G^0_{ads} = - RT \ln (55.5 \ K_{ads}) \qquad (10)$$

To calculate heat of adsorption (ΔH^0_{ads}) and entropy of adsorption (ΔS^0_{ads}) ln $K_{(ads)}$ vs. 1/T was plotted as shown in Fig.7(b). The straight lines were obtained with a slope equal to ($- \Delta H^0_{ads} / R$) and intercept equal to ($\Delta S^0_{ads} / R + \ln 1/55.5$). The values of equilibrium constant ($K_{(ads)}$), Standard free energy of adsorption(ΔG^0_{ads}), enthalpy of adsorption (ΔH^0_{ads}) and entropy of adsorption (ΔS^0_{ads}) are listed in Table-6.
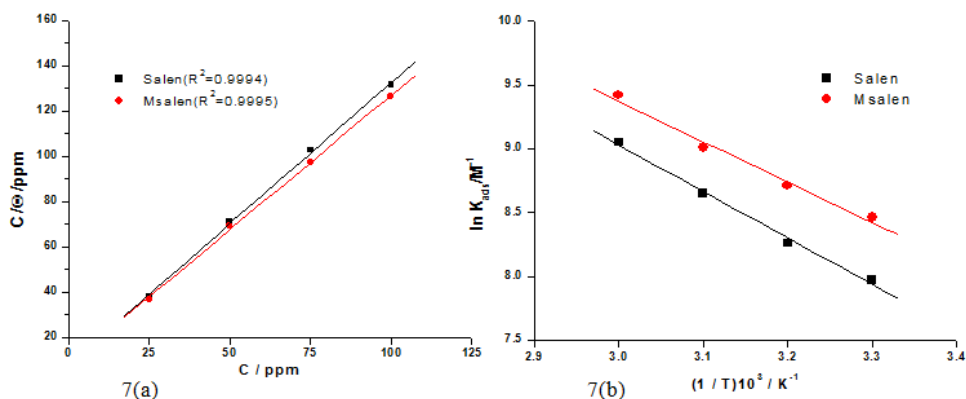

Figure. 7. (a) Langmuir adsorption isotherm plot and (b) Heat of adsorption isotherm plot for Salen and Msalen.

Table.6. Thermodynamic parameters for the adsorption of inhibitor in 1M HCl on AA6063 alloy surface at different temperature.

Inhibitor	Concentration (ppm)	Temperature (K)	K_{ads} ($10^3 M^{-1}$)	ΔG°_{ads} (kJmol^{-1})	ΔH°_{ads} (kJmol^{-1})	ΔS°_{ads} (Jmol^{-1})
Salen	100	303	8.49	-33	30.2	199
		313	5.7	-33		
		323	3.86	-33		
		333	2.9	-33		
Msalen	100	303	12.3	-34	26.3	190
		313	8.03	-34		
		323	6.09	-34		
		333	4.72	-35		

The negative values of standard free of adsorption indicated spontaneous adsorption of Schiff bases on aluminium alloy surface. The calculated standard free energy of adsorption values for the Schiff bases are closer to -40 kJ mole^{-1} and it can be concluded that the adsorption of Schiff bases on the aluminium surface is more chemical than physical one [47]. The sign of enthalpy and entropy of adsorption are positive and is related to substitutional adsorption can be attributed to the increase in the solvent entropy and to a more positive water desorption enthalpy. The increase in entropy is the driving force for the adsorption of the Schiff bases on the aluminium alloy surface.

The adsorption of Schiff base on the aluminium alloy surface can be attributed to adsorption of the organic compounds via phenolic and iminic groups in both cases. Among these two Schiff bases, the chelate effect of Msalen is greater than that of Salen. This is due to the presence of two electron donating groups of $-$OCH$_3$ in Msalen structure than Salen. The more efficient adsorption of Msalen is the result of electronegative oxygen atoms present in the Msalen compared to Salen Structure.

3.4 Scanning electron microscope (SEM)

Scanning electron microscopy of the inhibited and uninhibited metal AA6063 alloy samples are presented in Fig. 8. The SEM study shows that the inhibited alloy surface is found smoother than the uninhibited surface.
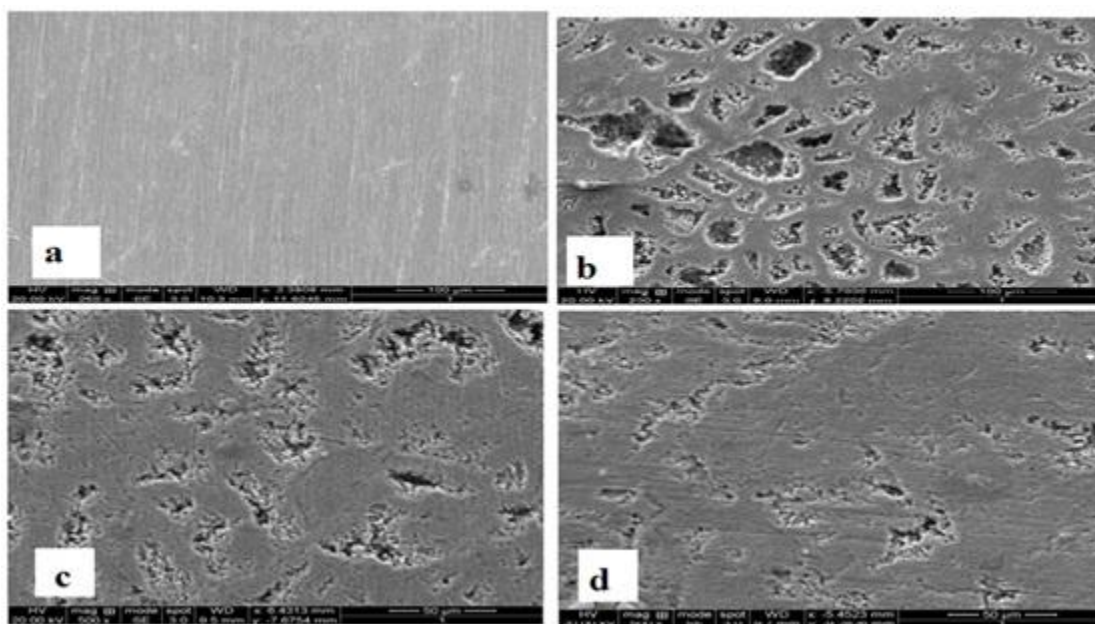

Figure. 8. Scanning electron micrographs of (a) Polished AA6063 alloy, (b) After immersion in 1M HCl for 2h, (c) After immersion in 1M HCl for 2h in presence of 100 ppm Salen and (d) After immersion in 1M HCl for 2h in presence of 100 ppm Msalen.

IV.   Conclusion

1. Potentiodynamic polarisation studies demonstrate the Schiff bases under investigation act as mixed type but predominantly cathodic inhibitors.
2. EIS measurements show that as the inhibitor concentration is increased, the charge transfer resistance increases and double layer capacitance decreases.
3. In weight loss studies, the inhibition efficiency (μ_{WL}%) of the Schiff bases increases with increase in inhibitor concentration, whereas decreases with increase in immersion time and temperature.
5. The inhibition efficiency obtained using weight loss, potentiodynamic polarisation, and EIS studies are in good agreement and in accordance to the order: Msalen > Salen for AA6061.
6. The adsorptions of Schiff bases on alloy surface in 1M HCl solution are governed by Langmuir adsorption isotherm.
7. The negative values of $\Delta G°_{ads}$ indicate that the adsorption of the Schiff base molecule is a spontaneous process and adsorption mechanism is typical of chemisorptions.

8. The CPE exponent (*n*) value increased with increase in inhibitor concentration is indicative of decrease in surface roughness of alloy surface.
9. Scanning Electron Microscopy (SEM) shows a smoother surface for inhibited alloy samples than uninhibited samples due to formation of protective barrier film.

References
[1]   Hatch JE (ed), Aluminum: properties and physical metallurgy. *American Society for Metals, Metals Park*, (1984) 424.
[2]   D. E. Tallman, G. Spinks, A. Dominis, G. G. Wallace, *J. Solid State Electrochem*. 6 (2002) 73.
[3]   Ergun U, Yuzer D, Emregul KC. The inhibitory effect of bis-2, 6- (3, 5-dimethylpyrazolyl) pyridine on the corrosion behaviour of mild steel in HClsolution. *Mater Chem Phys* 2008; 109: 492-9.
[4]   Hurlen T, Lian HH, Odegard OS, Valand TV. *Electrochim Acta* 1984; 29: 579-85.
[5]   Ebenso, E.E., Okafor, P.C., and Eppe, U.J., *Anticorr. Meth. Mat.*, 2003, vol. 50, no. 6, p. 414.
[6]   Blanc, C., Gastaud, S., and Mankowski, G., *J. Electrochem. Soc.,* 150(B) 2003, vol. 150, p. 396.
[7]   Mosaleva, A., Poznyok, A., Mozaleva, I., et al., *Electrochem.Comm.*, 2001, vol. 3, p. 299.
[8]   Klassen, R.D., Hyatt, C.V., Roberge, P.R., et al., *J. Canadian Metallurgical*, 2002, vol. 41, no. 1, p. 121.
[9]   Bazzi, L., Salghi, R., Zine, E., et al., *Can. J. Chem.,*2002, vol. 80, no. 1, p. 106.
[10]   Quafsaoui, W., Blanc, C.H., Bebere, N., et al., *J. Appl. Electrochem.*, 2000, vol. 30, p. 959.
[11]   Otmacic H, Stupnisek-Lisak E (2003) *Electrochim Acta* 48:985–991.
[12]   Ashish Kumar Singh, M . A. Quraishi*, Int. J. Electrochem. Sci., 7* (20120 3222-3241.
[13]   Fatemeh baghaei Ravari,Athareh Dadagarinezhad, Iran Shekhshoaei, *J.Chi. Chem. Soc. 55, N° 3* (2010) 328- 331.
[14]   Ashish Kumar Singh, M . A. Quraishi*, Int. J. Electrochem. Sci., 7* (20120 3222-3241.
[15]   Fatemeh Baghaei Ravari,Athareh Dadagarinezhad, Iran Shekhshoaei, *G.U Journal of Science,* 22(3), 175-182 (2009)
[16]   S. Patel, V. A. Panchal, G. V. Mudaliar, N. K. Singh, *Journal of Saudi Chemical society* (2011)xxx, xxx, xxx.
[17]   A. S. Patel, V. A. Panchal and N. K. Shah, *PRAJÑĀ - Journal of Pure and Applied Sciences, Vol. 18:* 7375 (2010).
[18]   T. Sethi, A. Chaturvedi, R. K. Upadhyaya, and S. P. Mathur, *Protection of Metals and Physical Chemistry of Surfaces,* 2009, *Vol. 45, No. 4,* pp. 466–471.
[19]   A. S. FOUDA, G. Y. ELEWADY, A. EL-ASKALANY, K. SHALABI, *ZAŠTITA MATERIJALA 51* (2010) broj 4, Scientific paper UDC:620.197.3:669.717.
[20]   Sanaulla Pathapalya Fakrudeen, Lokesh H. B, Ananda Murthy H. C, Bheema Raju V. B, *International Journal of Engineering Research and Applications (IJERA) ISSN: 2248-962,2* Vol. 2, Issue 5, September October 2012, pp.
[21]   Aluminum Association Publication T-8, *The Aluminum Association,* Washington, DC (1979).
[22]   T. Z. Yu, W. M. Su, W. L. Li, Z. R. Hong, R. N. Hua, M. T. Li, B. Chu and B. Li, *Inorg. Chem. Acta,* 2006, 359, 2246.
[23]   ASTM (2004) Standard practice for Laboratory Immersion Corrsion Testing of Metals G31-72.
[24]   A. Yurt, S. Ulutas, H. Dal, *Appl. Surf. Sci. 253* (2006) 919.
[25]   A. El-Sayed, Corros. *Prev. Control 43*(1996) 23.).
[26]   M. Metikos-Hukovic, R. Babic, Z. Grubac, *J. Appl. Electrochem. 28* (1998) 433.
[27]   C.M.A. Brett, *J. Appl. Electrochem. 20* (1990) 1000.
[28]   E.J. Lee, S.I. Pyun, *Corros. Sci. 37* (1995) 157.
[29]   C.M.A. Brett, *Corros. Sci. 33* (1992) 203.
[30]   K.F. Khaled, M.M. Al-Qahtani, *Mater. Chem. Phys. 113* (2009) 150.
[31]   A. Ehteram Noor, *Mater. Chem. Phys. 114* (2009) 533.
[32]   A. Aytac, U. Ozmen, M. Kabasakaloglu, *Mater. Chem. Phys. 89* (2005) 176.
[33]   T. Pajkossy, *J. Electronal. Chem. 364,* 111, (1994).
[34]   W.R. Fawcett, Z. Kovacova, A. Mtheo, C. Foss, *J. Electronal. Chem. 326***,** 91, (1992).
[35]   R. deLevi, *Electrochem. Acta 8 (*1963) 751.
[36]   H.J.W. Lenderink, M.V.D. Linden, J.H.W. De Wit, *Electrochim. Acta 38* (1989) 1993.
[37]   F. Mansfeld, C.H. Tsai, H. Shih, in: R.S. Munn (Ed.), *Computer Modeling in Corrosion,ASTM, Philadelphia, PA, 1*992, p. 86.
[38]   C.H. Hsu, F. Mansfeld, *corrosion 57* (2001) 747.
[39]   M.A Quraishi. Rawat *J (2001) Corrosion* 19: 273.
[40]   H. Ashassi-Sorkhabi, B. Shaabani, D. Seifzadeh, *Appl. Surf. Sci. 239* (2005) 154.
[41]   F. Mansfeld, Corrosion Mechanism, Marcel Dekkar, *New York, 1*987, p. 119.
[42]   Ashish Kumar Singh, M.A. Quraishi*, Corros. Sci. 52* (2010) 156.
[43]   E.A. Noor, A.H. Al-Moubaraki, Mater. *Chem. Phys. 110* (2008) 145.
[44]   A. Yurt, A. Balaban, S.U. Kandemir, G. Bereket, B. Erk, *Mater. Chem. Phys. 85*(2004) 420.
[45]   G.E. Badr, *Corros. Sci*. (2009), doi:10.1016/*j.cor sci*.2009.06.017.
[46]   T. Paskossy, *J. Electroanal. Chem. 364* (1994) 111.
[47]   A.Yurt, A. Balaban. S. Ustin Kandemir, G. Bereket. B. Erk, *Mateerials Chemistry and physics. 85* (2004) 420-426.